Scales of temporal and spatial variability of midlatitude land surface temperature

Konstantin Y. Vinnikov,[1] Yunyue Yu,[2] Mitchell D. Goldberg,[2] Ming Chen,[3] and Dan Tarpley[4]

[1] Scales of temporal and spatial variability of clear-sky land surface temperature (LST) in middle latitudes are empirically evaluated using data from satellite and land surface observations. We consider separately the time-dependent expected value, its spatial variations, weather-related temporal and spatial anomalies, and errors of LST observation. Seasonal and diurnal cycles in the time-dependent expected value of LST are found to be the main components of temporal variations of clear-sky LST. The scale of spatial variability in the expected value of LST is found to be much smaller than the scale of spatial variability of the weather-related signal. The scale of temporal autocorrelation of weather-related LST variations is found to be in a good agreement with our earlier preliminary estimate and equal to 3 d, which corresponds to the time scale of weather system variations. This weather-related signal in clear-sky LST is statistically the same as in surface air temperature (SAT) observations at regular meteorological stations. The scale of spatial autocorrelation of weather-related LST variations exceeds 1000 km, which is the spatial scale of synoptic weather systems. These estimates provide us with a basis for better understanding and interpretation of LST observations from past, current, and future geostationary satellites and polar orbiters.

Citation: Vinnikov, K. Y., Y. Yu, M. D. Goldberg, M. Chen, and D. Tarpley (2011), Scales of temporal and spatial variability of midlatitude land surface temperature, *J. Geophys. Res.*, *116*, D02105, doi:10.1029/2010JD014868.

1. Introduction

[2] Meteorologists have used land surface temperature (LST) in the energy balance equations for a long time, but they have only recently obtained a real opportunity to observe it from satellites. Unfortunately, desirable high spatial resolution infrared satellite observation of LST is possible only during clear-sky weather conditions. Microwave radiometers that can monitor LST in cloudy conditions are not yet able to provide sufficiently high spatial resolution. Of course, satellite observations should be able to monitor very strong diurnal/seasonal cycles in clear-sky LST. But, can LST anomalies be distinguished from these regular diurnal/seasonal variations, are these anomalies weather-related, can they be monitored? How large is land cover/topography-related spatial variability of LST? Is it masked by the weather-related signal? Unless we understand the scales of spatial and temporal variability of LST, we do not know if it is possible to accurately separate diurnal/seasonal cycles, weather-related signals, and land

cover/topography related variations in satellite observed LST. In this paper, we are trying to evaluate the scales of temporal and spatial variations of clear-sky LST using the available data from satellite and land surface observations. The effects of cloudiness on LST will be discussed in a separate paper. Results of analogous empirical studies of the scales of temporal and spatial variability of soil moisture [*Vinnikov and Yeserkepova*, 1991; *Vinnikov et al.*, 1996; *Entin et al.*, 2000] are often used for development and justification of requirements for satellite monitoring of soil moisture. Results of this study should be used same way for optimization of spatial and temporal resolution of satellite observations. Such statistical information is needed for developing a new approach to assimilation of satellite-observed clear-sky LST into weather analysis and prediction models. The same statistical information is needed for monitoring long-term climatic trends in LST. There are many applications of statistical information when we are trying to optimize monitoring of specific component of LST temporal or spatial change on the background of all other components of its variability.

[3] The boundary between atmospheric air and bare soil (or rocks) and/or land cover (water, vegetation, snow, roads, buildings, etc.) has complicated three dimensional shape. Physical temperature of the part of this boundary that contributes in emitting upward hemispheric flux of thermal radiation into atmosphere can be considered as LST or

[1]Department of Atmospheric and Oceanic Science, University of Maryland, College Park, Maryland, USA.
[2]NOAA/NESDIS, Camp Spring, Maryland, USA.
[3]IMSG at NOAA/NESDIS/STAR, Camp Spring, Maryland, USA.
[4]Short and Associates, Chevy Chase, Maryland, USA.

radiative skin temperature. Observed from different directions, this temperature has an angular anisotropy. The same type of definition can be used for land surface emissivity. A comprehensive discussion of LST and emissivity definitions for heterogeneous and non isothermical surfaces has been provided by *Becker and Li* [1995]. The main requirement is that a properly defined LST and emissivity should allow accurate computation of radiation and sensible heat fluxes between land surface and atmosphere.

[4] Standard meteorological observations usually do not include measurement of LST. An exception is the recently established Climate Reference Network (CRN) in the United States, which provides hourly averages of LST observed by narrow angle infrared radiometers, blackbody calibrated. More reliable LST data with higher (3 min averages) temporal resolution can be obtained from upward (I_u) and downward (I_d) broadband infrared hemispheric fluxes observed at the Surface Radiation Network (SURFRAD) in the United States and analogous stations in other countries [*Augustine et al.*, 2000]. Assuming that land surface emissivity (*E*) is known, an efficient LST can be estimated from traditionally used equation $LST = \{[I_u-(1-E)I_d]/(sE)\}^{0.25}$, where *s* is Stefan-Boltzmann constant. Unfortunately, neither CRN nor SURFRAD stations observe cloudiness. Nevertheless, data from these stations can be combined with geostationary satellite observations for cloud detection. A simple Russian technique of LST observations uses a liquid-in-glass thermometer laying horizontally, half buried in bare soil, in an observational plot. When the ground is snow covered, the thermometer is placed on the snow surface and the temperature of the snow cover is measured [*Razuvaev et al.*, 2007]. Such observations may be considerably biased when the thermometer is exposed to direct solar radiation and cannot be accurately used for studying daytime clear-sky LST.

[5] Downward looking pyrgeometers at SURFRAD stations are installed at height of 8 m above land surface. This footprint is much smaller compared to footprints of satellite radiometers used in this study: ~4 km at nadir for GOES-10 Imager and ~90 m for TERRA ASTER observations.

[6] Surface air temperature (SAT) at SURFRAD stations is observed by a Sun-shielded thermistor installed near the top of the 10 m tower. It is usually observed at meteorological stations at standard heights of 1.5 m or 2 m above land surface. This difference is not significant for this study. As all other SURFRAD variables, SAT is averaged for 3 min time intervals. Efficient spatial averaging of SAT data depends on wind speed and is of the order of 1 km. We will see later that this scale is much smaller than the scale of spatial autocorrelation of weather-related signal in this variable.

2. Method

[7] The method used here to retrieve clear-sky LST from observations of geostationary satellite GOES-10 over the continental part of the United States is described by *Yu et al.* [2008, 2009]. The temporal increment in this LST data is 1 h or longer when cloudiness does not permit satellite observations of the land surface. Temporal and spatial variability of meteorological variables is often studied using a theory of random stationary processes and fields. It is well established that the regular autocorrelation function of meteorological variable decreases with an increase of time lag or distance between observations [*Czelnai et al.*, 1976; *Kagan*, 1997]. The distances or lags at which spatial or temporal autocorrelation functions approach zero (or statistically insignificant level) are used here to characterize scales of spatial or temporal variability. This definition of LST variability scales is different than used for soil moisture with exponential correlation functions [*Vinnikov et al.*, 1996; *Entin et al.*, 2000]. The estimates show that correlation functions of LST are not quite exponential.

[8] We assume that long-term climatic trends are insignificant in satellite and surface observed LST and SAT data used in our analysis. There were no instrumental problems or other events that made the observed records inhomogeneous. We understand that interannual and interdecadal climate variability is not well represented in the data used here. Let us denote satellite observed LST as $f(t, x, y)$, where *t* is time; *x* and *y* are horizontal coordinates. As discussed by *Vinnikov et al.* [2008], we present all temporal variations of LST as a sum of three independent components. The leading components of temporal variability of LST in the middle latitudes are the systematic diurnal and seasonal cycles denoted as $F(t, x, y)$ which is the time-dependent expected value of this temperature. The observed value of LST also contains the weather anomaly (weather-related signal), $f'(t, x, y)$, and the random error of observation, $\varepsilon(t, x, y)$. From that, we can write

$$f(t,x,y) = F(t,x,y) + f'(t,x,y) + \varepsilon(t,x,y). \quad (1)$$

Random errors of observations at different locations and at different times are assumed to be uncorrelated and can be characterized by their variance

$$\overline{\varepsilon(t,x,y)\varepsilon(t + \Delta t, x + \Delta x, y + \Delta y)}$$
$$= \begin{cases} \delta^2(t,x,y) & for \quad \Delta t = \Delta x = \Delta y = 0, \\ 0 & for\, \Delta t \neq 0 \quad or \quad \Delta x \neq 0 \quad or \quad \Delta y \neq 0. \end{cases} \quad (2)$$

For the same satellite radiometer, the dependence of standard error $\delta(t, x, y)$ on horizontal coordinates is weak and can be ignored for nearby pixels. We also ignore the dependence of standard error on time, but such errors may vary between day and night, as well as between wet and dry atmospheric conditions. For a stationary instrument at a surface station, random error of observation is considered to be statistically independent of errors of other instruments at the same or at other locations.

[9] Temporal variations of weather-related signal (anomalies) at a location (x, y) can be characterized statistically by the lag-covariance function:

$$R_f(\tau,x,y) = \overline{f'(t,x,y)f'(t + \tau,x,y)} = \sigma_f^2(x,y)r(\tau). \quad (3)$$

Here $r_f(\tau)$ is a temporal lag-correlation function that depends on time lag τ, and $\sigma_f(x, y)$ is standard deviation of $f'(t, x, y)$ that depend on horizontal coordinates and has weak diurnal and seasonal cycles that can be ignored in (3) based on estimates discussed in the section 4 below.
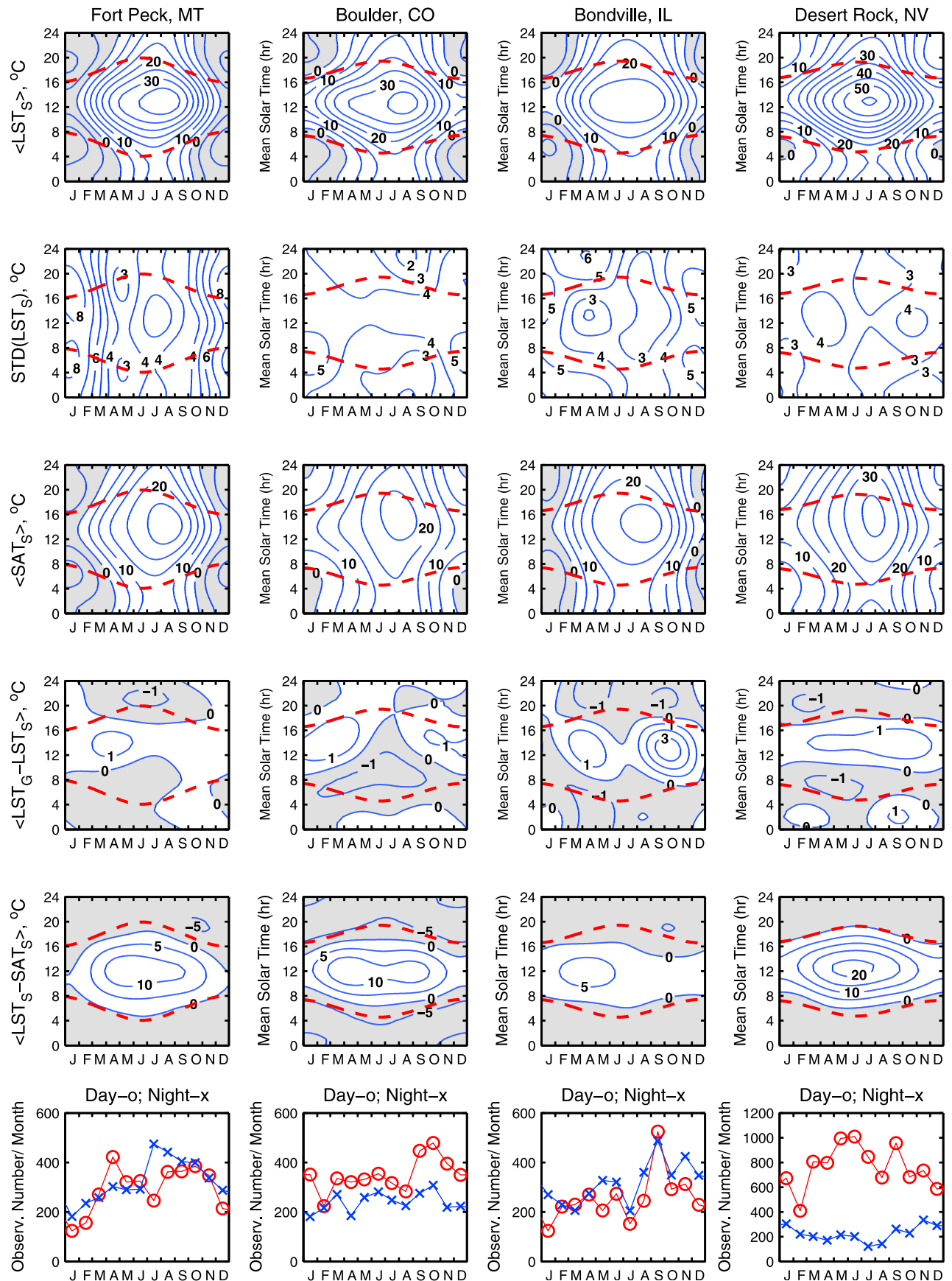
Figure 1

Table 1. List of SURFRAD Stations

SURFRAD Station Name	Land Cover Type	Location		Number of Observations	Surface Emissivity [*Snyder et al.*, 1998]	Bias[a] (°C)
		Lat. (°N)	Lon. (°W)			
Fort Peck, Montana	Grassland	48.31	105.10	7,443	0.984	−2.1
Boulder, Colorado	Cropland	40.13	105.24	7,083	0.982	−1.8
Bondville, Illinois	Cropland	40.05	88.37	6,884	0.982	−1.3
Desert Rock, Nevada	Open Shrub Land	36.63	116.02	11,870	0.957	−1.9

[a]The bias is defined as $\ll LST_{GOES-10} - LST_{SURFRAD} \gg$.

[10] Spatial variations of the weather-related signal can be characterized statistically using a spatial autocovariance function:

$$R_f(x,y,\rho) = \overline{f'(t,x,y)f'(t,x+\Delta x, y+\Delta y)}$$
$$= \sigma_f(x,y)\sigma_f(x+\Delta x, y+\Delta y)r_f(\rho), \qquad (4)$$

where $\sigma_f(x,y)$ is standard deviation of the same $f'(t,x,y)$ as in (3), $\rho = \sqrt{\Delta x^2 + \Delta y^2}$ is a distance and $r(\rho)$ is the spatial autocorrelation function.

[11] The signal $F(t,x,y)$, which represents systematic seasonal and diurnal cycles, is spatially and temporally dependent. The following simple mathematical model, which is applicable for its approximation, was tested for LST and other meteorological variables by *Vinnikov and Grody* [2003] and *Vinnikov et al.* [2004, 2006, 2008]:

$$F(t,x,y) = \sum_{k=-K}^{K}\sum_{n=-N}^{N} a_{kn}(x,y)e^{i\pi t\left(\frac{n}{T}+\frac{k}{H}\right)}. \qquad (5)$$

This expression represents a result of amplitude modulation of a diurnal cycle variation, approximated by K Fourier harmonics with a period of $H = 1$ d, by an annual cycle variation, approximated by N harmonics with period $T = 365.25$ d. The $a_{k,n}$ coefficients can be estimated using ordinary or generalized least square techniques. $F(t,x,y)$ is a periodic function of two periods H and T and can be displayed in a two-dimensional plot as a function of two arguments, which are time intervals from the beginning of a day and from the beginning of a year.

[12] The dependence of $F(t,x,y)$ on horizontal coordinates cannot be studied using observations of existing stations. There are not many pairs of LST stations with small distances between them. Locations of LST observing stations are usually chosen to be representative for their surrounding region. Observations of such stations do not represent the main part of spatial variability of $F(t,x,y)$, which depends on spatial variations of topography and land cover. For example, outside of the tropics there is a well known difference in the temperature regime on southern and northern slopes of hills. For this reason, observation plots are never chosen on a slope, and are usually placed at horizontal locations. At the same time, vegetation at observational plots usually does not represent agricultural

activity in the vicinity of stations. Real spatial variability in the expected value of clear-sky LST $F(t,x,y)$ can be seen only from very high resolution satellite and aerial images. This component of spatial variability in the expected value can be characterized statistically using a geostatistical technique of structure functions. For spatially homogeneous and isotropic random fields, the structure function can be defined as the mean square of the difference between two values of our variable as a function of a distance (ρ) between points:

$$b_F(t,\rho) = \overline{(F(t,x,y) - F(t,x+\Delta x, y+\Delta y))^2}. \qquad (6)$$

The relationship between the structure and covariance functions can be found in the work of *Kagan* [1997]. We will see later that the scale of the weather-related spatial variability of LST is much larger than the scale of spatial variations in the expected value of LST. Reasonable estimates of $b(t,\rho)$ for relatively small distances, when $f'(t,x,y) \approx f'(t,x+\Delta x, y+\Delta y)$, can be obtained from high-resolution satellite observations of LST. Using equations (1), (2), and (5) and the assumption that the standard error of this observation does not depend on coordinates $\delta^2(x,y) = \delta^2 = const$, we get

$$b_F(t,\rho) \approx \overline{(f(t,x,y) - f(t,x+\Delta x, y+\Delta y))^2} - 2\delta^2. \qquad (7)$$

This means that random errors of LST observation do not affect estimates of the spatial scale of $F(t,x,y)$ variations and observed $f(t,x,y)$ can be used instead of the not observable $F(t,x,y)$.

3. Data

[13] Hourly data used for studying temporal variations of LST are from three (2001, 2004, and 2005) years of observations of four SURFRAD stations listed in Table 1, and GOES-10 satellite retrieved LST at the locations of these stations. The statistical algorithm that has been applied to eliminate cloud contaminated data uses both satellite and SURFRAD observations. This algorithm is more objective than the earlier one used by *Vinnikov et al.* [2008], and detects nighttime cirrus cloudiness more accurately than the algorithm that does not use satellite observations [*Long and Turner*, 2008; *Long et al.*, 2006; *Long and Ackerman*,

Figure 1. Time-dependent expected value: first row depicts $\langle LST_S \rangle$ of SURFRAD observed LST_S; second row depicts $STD(LST_S)$, standard deviation of this temperature; third row depicts $\langle SAT_S \rangle$, SURFRAD surface air temperature; fourth row depicts $\langle LST_G-LST_S \rangle$, systematic difference between GOES-10 and SURFRAD observed LST; fifth row depicts $\langle LST_S-SAT_S \rangle$, systematic difference between SURFRAD observed LST and SAT. Dashed lines display sunrise and sunset times. Sixth row depicts monthly numbers of available daytime and nighttime clear-sky observations at each station.

2000]. Table 1 also contains the total number of available clear-sky observations for each of these stations. The SURFRAD stations provide LST averages for each 3 min interval. Each clear-sky satellite LST has been collocated with the corresponding ground station and time matched to the nearest 3 min surface observation. Only coincided in time satellite and surface data that exist in both data sets has been used. Additional information about number of clear-sky observations for daytime and nighttime for each month is given in the sixth row of the panels in Figure 1. At nighttime, there is no visible cloud reflectance data for use in cloud screening algorithm. So, tighter thresholds based on infrared channels are applied to minimize cloud-contaminated LST. This explains the fewer number of night-time clear-sky data at the Desert Rock SURFRAD station.

[14] GOES-10 observed LST has been retrieved using a split window algorithm by *Ulivieri and Cannizzaro* [1985] as modified by *Yu et al.* [2009]. LST at the SURFRAD stations is computed using observation of broadband upward and downward infrared fluxes as has been explained in section 1. The surface emissivities by *Snyder et al.* [1998], which are dependent on land cover type, are shown in Table 1. The same emissivities have been used to compute LST from satellite and surface observations. Seasonal cycles and differences in emissivities of different crops are ignored. These assumptions do not influence results of this scale analysis.

4. Seasonal and Diurnal Cycles in the Expected Value of LST

[15] Earlier, *Vinnikov et al.* [2008] used one (2001) year of independent observations of LST from two geostationary satellites (GOES-8 and GOES-10) at the locations of five SURFRAD stations to evaluate the time-dependent expected value. It was found that systematic differences between these three estimates themselves have seasonal and diurnal cycles and are comparable in magnitude with random errors of observation. Here we use three years (2001, 2004 and 2005) of LST observations at four SURFRAD stations and one (GOES-10) satellite with a new objective statistical algorithm to filter out cloud-contaminated satellite and surface-measured LSTs. Estimates of diurnal/seasonal variations, the term $F(t, x, y)$ in (1), of SURFRAD observed clear-sky LSTs (Figure 1, first row) update estimates discussed by *Vinnikov et al.* [2008]. These new estimates better represent interannual variability of the LST because they are based on three years of observation. The longer time series provides an opportunity to estimate the diurnal/seasonal variations of standard deviations (Figure 1, second row). To obtain these estimates, the approximation (5) has been applied to the time series of squared residuals $(f''(t, x, y) + \varepsilon(t, x, y))^2$, as has been done earlier by *Vinnikov and Robock* [2002] and *Vinnikov et al.* [2002, 2004]. The computed variance is overestimated because it is equal to a sum of real LST variance and variance of observation error. Fortunately, the errors are significantly smaller than weather-related fluctuations [*Vinnikov et al.*, 2008]. Standard deviations for GOES-10 observed LSTs are not shown here because they reveal the same diurnal/seasonal patterns and values very close to values to those presented in Figure 1. However,

these patterns vary from station to station and cannot be easily interpreted.

[16] The expected value of annual average LST is equal to the coefficient α_{00} in (5). Mean differences of annual LST temperatures estimated from the observations of GOES-10 and SURFRAD stations are given in Table 1 as $\ll$LST$_G$-LST$_S\gg$. The estimations show that the GOES-10 observed LST is systematically underestimated, by about 1.8°C, compared to LST observed at the four SURFRAD stations. If annual biases in expected values are removed, we still have a diurnal/seasonal pattern of systematic differences between satellite and surface observed LST (Figure 1, fourth row) denoted as $\langle$LST$_G$-LST$_S\rangle$. These differences manifest angular anisotropy of LST field and depend on viewing and illumination geometry. They also depend on differences in land cover of a pyrgeometer footprint at SURFRAD stations, that never have large trees and agricultural activity, and the much larger footprint of the satellite pixel.

[17] The expected value of surface air temperature (SAT) at the SURFRAD stations (Figure 1, third row) is analyzed and compared to the LST. Again, we use SAT observations which are simultaneous with satellite and SURFRAD clear-sky LST data. Seasonal and diurnal cycles of the LST$_S$ are significantly larger than those of the SAT$_S$. Mean differences, $\langle$LST$_S$-SAT$_S\rangle$, of these temperatures at clear-sky conditions (Figure 1, fifth row) are positive during daytime (LST > SAT) and negative at nighttime (LST < SAT) and are dominated by much larger daytime differences, LST$_S$-SAT$_S \approx$ 5–20°C. By magnitude, these differences are several times larger in daytime than nighttime. The largest systematic differences, LST$_S$-SAT$_S \geq$ 20°C, are observed at Desert Rock, NV, which has a very dry desert climate and little or no vegetation or water.

5. Scales of Temporal Autocorrelation of Weather-Related LST Variations

[18] Empirical estimates of temporal lag-correlation functions of residuals, $f(t, x, y) - F(t, x, y) = f'(t, x, y) + \varepsilon(t, x, y)$, which are weather-related anomalies of the GOES-10 observed LST$_G$, the SURFRAD observed LST$_S$, and the SURFRAD observed SAT$_S$, and are contaminated by random errors of measurements, are shown in Figure 2. The traditional Fast Fourier Transformation (FFT) technique could not be applied because of large time gaps in the data caused by cloud cover. So, we estimated and plotted correlation coefficients for hourly time lags $|\tau| = 1, 2, 3 \ldots,$ 168 h using all pairs of observations inside of the hourly time intervals $[\tau - 0.5, \tau + 0.5]$. As was found by *Vinnikov et al.* [2008] from one year data, the scale of the temporal autocorrelation of the weather-related component of clear-sky LST variation T_f is about 3 d.

$$R_f(\tau, x, y) = \sigma_f^2(x, y) r_f(\tau), \text{ if } \tau \geq T_f \text{ then } r_f(\tau) \approx 0, T_f \approx 3 \text{ dy}.$$

(8)

We come to the same conclusion looking at lag-correlation LST estimated from 3 years of satellite and SURFRAD LST data. Only one station, Desert Rock, NV, shows the existence of long-term interannual variability. We also estimated lag-correlation functions for the SAT for clear-sky conditions and found that autocorrelation functions of clear-
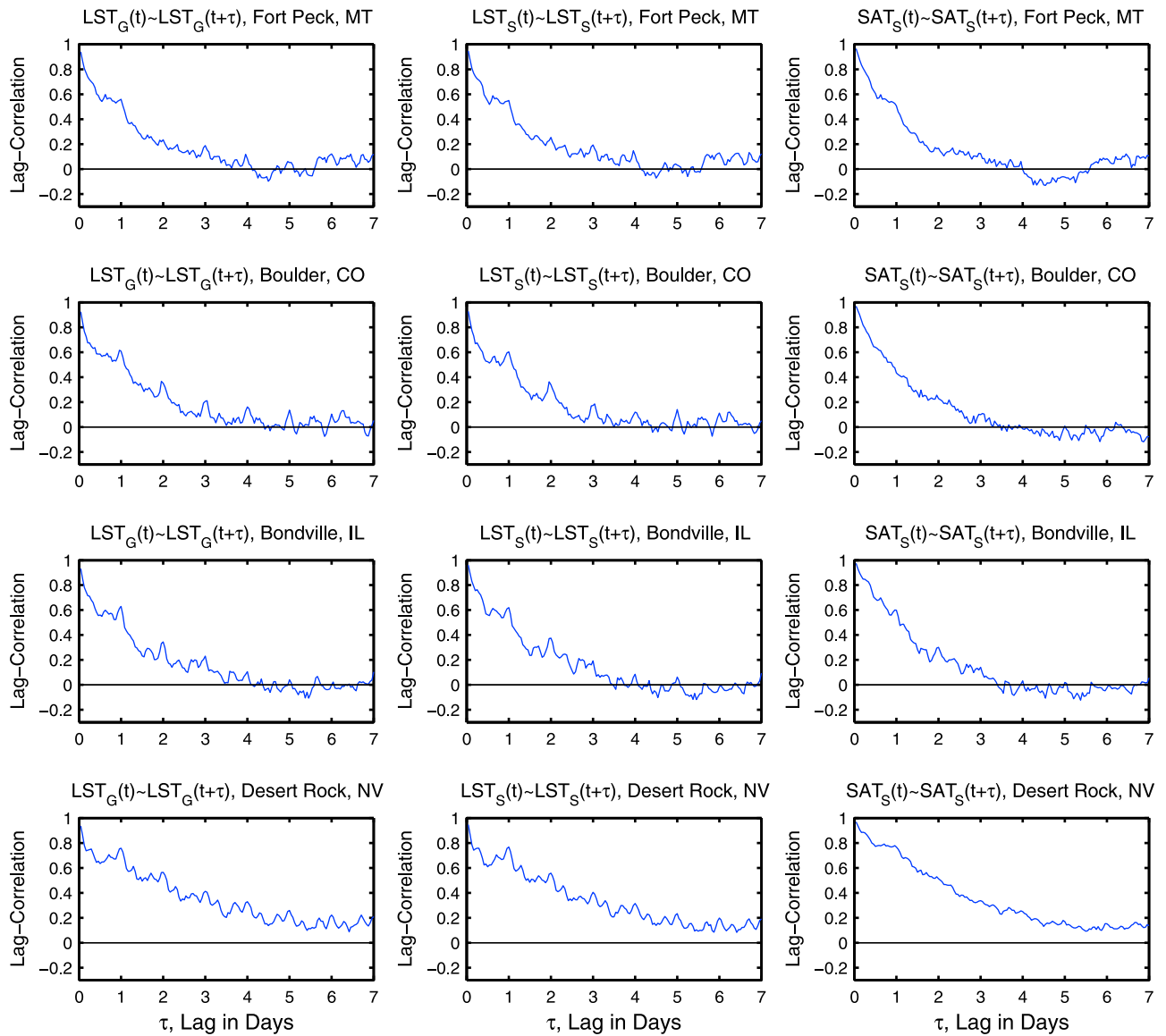
Figure 2. Lag-correlation functions of satellite GOES-10 observed LST_G, SURFRAD observed LST_S, and SURFRAD observed SAT_S. These estimates are biased (underestimated) because of random errors of observation.

sky SAT_S and LST_S are almost indistinguishable. Does this mean that LST and SAT carry the same weather-related signal? To answer this question we evaluated the temporal cross-correlation functions of the GOES-10 observed LST_G and the SURFRAD observed LST_S and SAT_S for the same stations, which are presented in Figure 3. These three cross-lag-correlation functions for each of the stations look the same and they are not very different when compared to the autocorrelation functions presented in Figure 2. Small differences in the cross-correlations reflect differences in errors of observations, which are not very large. Cross-correlations of two LST time series, observed from the GOES-10 and from the SURFRAD stations are totally symmetric. An asymmetry in estimates of cross-correlation functions of the LST and the SAT can be seen but it is very small. One should expect from simple physics that changes in clear-sky LST should precede changes in SAT. It looks as if temporal

variations in both of these variables at each location are primarily modulated by changes in synoptic weather systems. This means that useful information in clear-sky LST observations, beyond that of systematic seasonal and diurnal cycles, is mostly the same as in routine observations of temporal variations of SAT at regular meteorological stations. Note that this conclusion is for clear-sky weather only. The life cycle of moving weather systems is about one week and that is longer than the time scale of LST and SAT perturbations at clear skies at fixed locations.

6. Scales of Spatial Autocorrelation of Weather-Related LST Variations

[19] Spatial autocorrelation functions of surface air temperature are well studied. A well-known comprehensive review on the statistical structure of meteorological fields
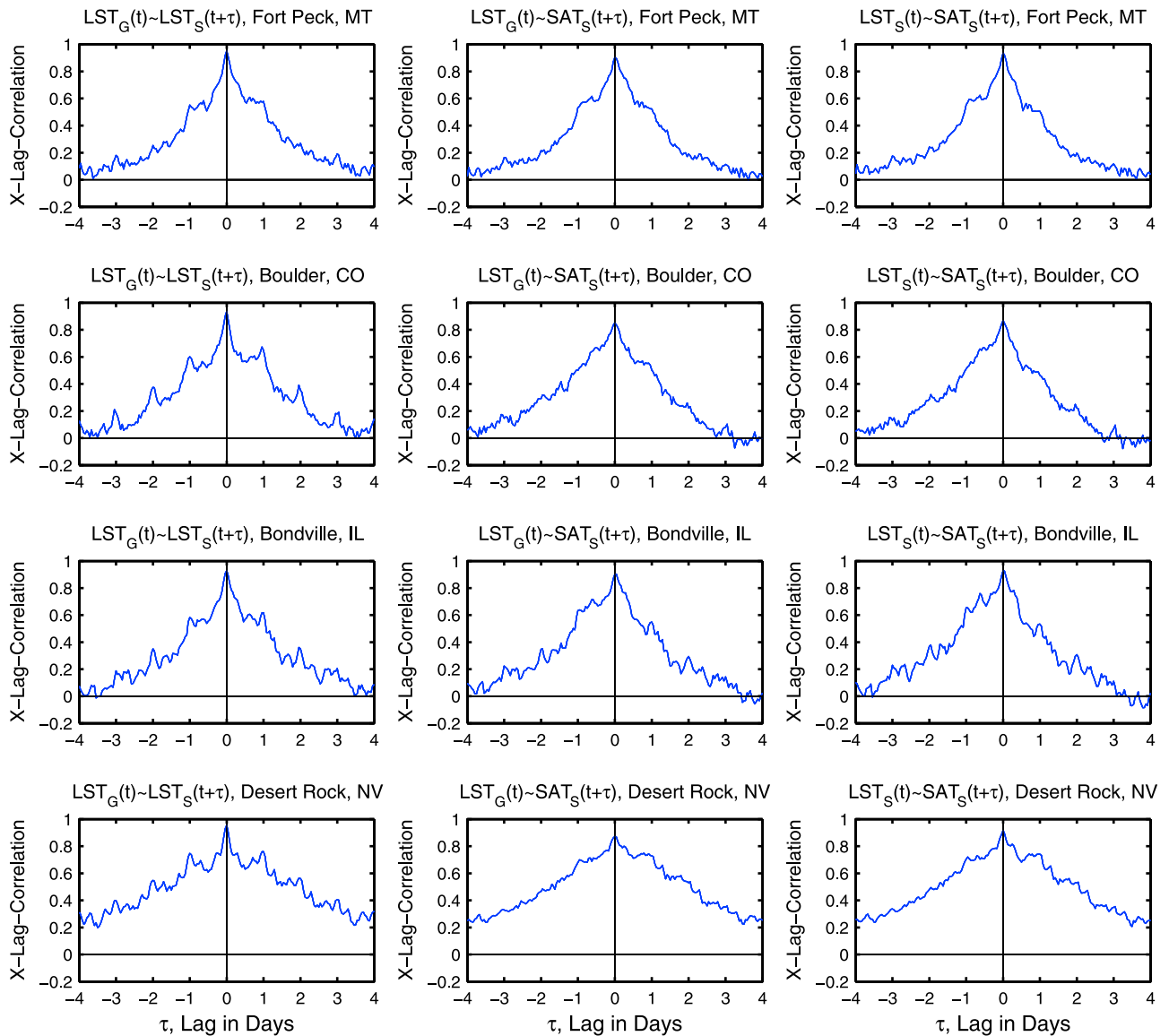
Figure 3. Cross-lag-correlation functions of GOES-10 observed LST_G, SURFRAD observed LST_S and SURFRAD observed SAT_S. These estimates are biased (underestimated) because of random errors of observation.

discusses results of 20 related publications [*Czelnai et al.*, 1976]. There is no need to repeat these studies. The scales of spatial autocorrelation of SAT are found to be generally larger than 1000 km at different times of day for all seasons at most more or less homogeneous midlatitudinal regions of Europe and Asia [*Rakoczi et al.*, 1976]. *Hrda* [1968] showed that for distances up to ~150 km spatial autocorrelation functions of SAT under clear-sky conditions are significantly larger than for all sky conditions and overcast sky conditions. This means that scale of spatial autocorrelation of SAT for clear-sky conditions should be larger than one estimated for all sky conditions. The same is expected for midlatitude America. Since the scales of temporal autocorrelation of weather-related variations in LST and SAT are equal, the scales of spatial autocorrelation should be equal for weather-related variations in LST and SAT fields. This is because the temporal local weather signal is

generated by the moving pattern of the same weather systems. The scale of spatial autocorrelation of clear-sky LST can be approximately evaluated from estimates of the scale of temporal autocorrelation obtained in section 5. Using a mean speed of 5 to 10 m/s for the Northern hemisphere midlatitudinal weather systems propagation [*van den Dool*, 2007] we have to multiply this speed by the scale of temporal lag-correlation, which is 3 d. The resulting estimate of a distance at which the spatial autocorrelation of the LST field is near zero was found to lay somewhere between 1300 km and 2600 km. On the basis of these estimates we can conclude that the scale of spatial autocorrelation in the weather related component of clear-sky LST variations exceeds 1000 km. This is important for understanding that as long as the footprint of a satellite radiometer is much less than the scale of weather systems, less than 10 km for example, it can be efficiently used for monitoring the
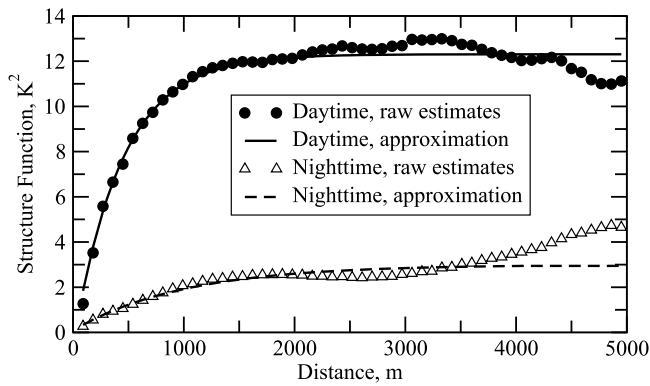
Figure 4. Empirical estimates and approximations of structure functions of $F(t, x, y)$ for two satellite high-resolution LST images made by ASTER in the vicinity of the Bondville, Illinois, SURFRAD station. Nighttime image obtained on 12 March 2004 at ~2230, and daytime image obtained on 19 September 2004 at ~1030 local solar time. Exponential functions used for approximation $b_F(\rho)$ do not behave well for distance $\rho = 0$ and are shown in this figure for visualization of expected dependence of structure functions on ρ for large distances.

weather-related spatial signal in the LST field. We can summarize this as

$$R_f(\rho) = \sigma_f^2 r_f(\rho), \text{ if } \rho \geq L_f \text{ then } r_f(\rho) \approx 0, L_f > 1000\,\text{km}. \quad (9)$$

More accurate empirical estimates of spatial autocorrelation functions of the weather-related component of LST variability can be obtained using not less than one full year of satellite LST observations for regions with linear size of about a few thousand km. Time-dependent expected value should be computed for each location and subtracted from observed LST to compute weather-related anomalies $f'(t, x, y)$. This time-consuming task is for future research.

7. Scales of Spatial Variability in the Expected Value of LST

[20] The time-dependent expected LST, $F(t, x, y)$, depends on horizontal coordinates. By default, the main goal of satellite observations of LST is to monitor its spatial and temporal weather-related variations. From this point of view, the large spatial and temporal variation of expected value of LST interferes with the weather signal and makes it unrecognizable and undetectable in observed data. So we need information about scales of variability of both, weather signal and expected value. Let us assume that $F(t, x, y)$ can be considered as a random, homogeneous and isotropic function of coordinates x and y at each time t. The structure function defined in equations (6) and (7) for such a field at time t depends on the distance between two arbitrarily selected points and can be estimated using single high-resolution spatial images of LST for the selected region. An example of the structure function estimates for the vicinity of the SURFRAD station Bondville, Illinois, is given in Figure 4. These estimates are for daytime and nighttime observations of LSTs derived from Advanced Spaceborne Thermal Emission and Reflectantion Radiometer (ASTER)

data, a relatively high (90 m at nadir) spatial resolution radiometer onboard Terra, a satellite launched in 1999 as part of NASA's Earth Observation System (EOS). Both curves in Figure 4 show the same, close to $L_F \approx 1.5$–2 km, distance of saturation of the structure functions, which correspond to the scale of spatial autocorrelation. Spatial variability of the expected value of LST has two main sources, topography and pattern of vegetation cover. The primary cause of daytime spatial variation in LST is the fraction of the surface covered with active transpiring vegetation. Evapotranspiration decreases the amount of net radiation at the surface that goes into specific heat and increases the latent heat flux from the surface. For this reason vegetated surfaces are substantially cooler than bare soil and dead vegetation. At night, without insolation to supply large surface energy fluxes, surface LST is less spatially variable at the local scale although some nighttime spatial variation in LST can be caused by concentration of cold air in low spots. Nevertheless, we expect that the variance and the shape of the structure functions change with a diurnal cycle, not the distance at which the structural functions are saturated. Generally, the main scale of spatial autocorrelation (L_F) should be approximately the same at daytime and at nighttime because of its dependency on the topography and vegetation pattern which change slowly. Our preliminary estimates show that $L_F \ll L_f$. By converting the structure functions into covariance functions we can summarize

$$R_F(t, \rho) = \sigma_F^2(t) r_F(t, \rho), \text{ where } r_F(t, \rho) \approx 0 \text{ for } \rho \geq L_F. L_F \ll L_f. \quad (10)$$

Note that variances of observation errors in structure functions estimates shown in Figure 4 are negligibly small compared to spatial variance of expected value of LST itself.

8. Concluding Remarks

[21] Observed spatial and temporal variations in LST can be considered as a sum of three independent components shown in equation (1); each has its own temporal and spatial variability.

[22] First, $F(t, x, y)$ is the time-dependent expected value of LSTs. At each location (x, y) it represents climatology of diurnal and seasonal cycles of LST. Its temporal variation is the largest signal in the observed LSTs. The change rate of mean LST in the diurnal cycle at some of the stations reaches 5–6°C/h. According to its temporal cycles for diurnal and seasonal variations, once we accumulate enough data to accurately estimate the cycle signal, no more observations of LST are needed to know its expected value each day of a year and at each time of day. The proposed approximation for this function as described in equation (5) is well tested, though it contains too many empirical parameters (e.g., 25 for $K = N = 2$) to be easily determined at each location. Fortunately, many of them are negligibly small and statistically insignificant. Because the LST field has angular anisotropy, the functions $F(t, x, y)$ estimated for the same location from observations of two American geostationary satellites GOES-EAST and GOES-WEST are not the same [*Vinnikov et al.*, 2008]. Sooner or later, multiyear LST observations from each geostationary satellite should be used to evaluate time-dependent expected value of LST

at each clear-sky land pixel in the field of view of the satellite radiometers. Observations of meteorological satellites in polar orbits are not able to provide sufficient information about the diurnal cycle of LST and are more or less useless for evaluation of the time-dependent expected value $F(t, x, y)$.

[23] Spatial variations in $F(t, x, y)$ are mostly caused by the topography and vegetation patterns. It is recognized that they can be studied and evaluated statistically using a technique that is traditional in geology and geostatistics. Our analysis is based on assumption that at distances less than a few tens of km at each specific time of a day and day of a year, $F(t, x, y)$ can be considered as a homogeneous and isotropic random field of horizontal coordinates. In this assumption it is found that the scale of spatial autocorrelation in such a field in vicinity of selected SURFRAD station does not exceed a few km in distance. So, the initial assumption is acceptable. This scale dependence on time of day or season still should be studied for different types of topography and land cover. Spatial variance of $F(t, x, y)$ has very strong diurnal (and seasonal) cycles with its minimum at nighttime. Scales of this spatial variability are close to the size of footprints of radiometers used for LST observation with current and future generations of geostationary satellites. Many problems of characterization and optimization of satellite instruments can be formulated and solved using such statistics and theory of random meteorological fields [*Kagan*, 1997]. Among them are evaluations of the effects of pixel size and uncertainties in pixel geolocation. If the size of a satellite radiometer footprint is large enough, a significant part of this small-scale spatial variability in the expected value is suppressed by spatial averaging over the pixel area. The scale of such microclimatic spatial variability of LST is much smaller than the synoptic-scale LST variations and even smaller than the size of GOES-10 footprint. Pixel averaged signal is close to LST signal observed at well selected area representative observational plots of surface stations.

[24] Subtracting the expected $F(t, x, y)$ from the observed LST value $f(t, x, y)$ we obtain a combination of the weather-related component of LST temporal and spatial variability $f'(t, x, y)$, and a random error $\varepsilon(t, x, y)$. We found that the time scale of temporal variability of LST is about 3 d in midlatitudes of North America. We showed that the weather-related signal in time series of clear-sky LSTs is almost the same (statistically indistinguishable) as that we see in time series of clear-sky SATs. We also concluded that the scale of spatial variations in weather-related clear-sky LST variability exceeds 1000 km. This means that the current spatial resolution of satellite LST observations from polar and geostationary orbits is useful for monitoring of the weather-related spatial patterns of LST variability. However, weather-related signal $f'(t, x, y)$ cannot be separated from diurnal cycle in observation of polar orbiters without knowing $F(t, x, y)$.

[25] Because of measurement errors, lag = 0 correlation coefficients between GOES-10 and SURFRAD observed LST in Figure 3 are less than one (0.93–0.96). Assuming, as has been shown earlier [*Vinnikov et al.*, 2008], standard errors of the LST observations from GOES-10 satellite and SURFRAD stations are approximately equal, we conclude that variances of observation errors do not exceed 5% of the variance of weather-related signal at the locations of four selected SURFRAD stations. This is an excellent accuracy for the LST weather signal monitoring in middle latitudes.

[26] As noted earlier the satellite observes LST only under clear-sky conditions which mostly is over high-pressure regions. Total variability of LST for all sky conditions is much larger than for clear-sky only. Satellites cannot measure LST for cloud contaminated pixels. This makes satellite retrieved LST fields discontinuous and more difficult to assimilate in weather prediction models because of large difference in regimes of LST at clear and overcast skies. (Many other satellite products are discontinuous, satellite soundings and winds for example, yet they are assimilated in model very well). In many cases, SAT observed at existing networks of meteorological stations can be used as proxy for LST in overcast sky conditions. For clear-sky, we found that weather-related signal in LST and SAT fields are statistically very close. This means that SAT observations and satellite retrieved LST should be assimilated together. A new approach for such assimilation should be developed. The difference between clear-sky LST and SAT provides valuable information on stability of the atmospheric boundary layer. Dry atmospheric conditions and clear skies usually cause extremely low LST at nighttime and extremely high LST in result of solar heating in the early afternoon. Such information is very important in for realistic high-resolution modeling of the chemical cycles of such atmospheric pollutants as ozone and other physical and chemical processes in atmospheric boundary layer. LST for clear-sky conditions have special importance and have to be monitored even in absence of such information for cloudy sky.

[27] The main result of this study consists of evaluation of all major components of temporal and spatial variability of midlatitude satellite observed LST. We understand now their physical nature and scales of their autocorrelation. The same approach can be applied to study statistical properties of LST field in equatorial, tropical, subtropical and high latitudes for different land covers and different landscapes include mountains. More research for midlatitude LST is also needed.

References

Augustine, J. A., J. J. DeLuisi, and C. N. Long (2000), SURFRAD-A National Surface Radiation Budget Network for Atmospheric Research, *Bull. Am. Meteorol. Soc.*, *81*, 2341–2357, doi:10.1175/1520-0477 (2000)081<2341:SANSRB>2.3.CO;2.

Becker, F., and Z.-L. Li (1995), Surface temperature and emissivity at various scales: Definition, measurement and related problems, *Remote Sens. Rev.*, *12*, 225–253, doi:10.1080/02757259509532286.

Czelnai, R., L. S. Gandin, and W. I. Zachariew (Eds.) (1976), *Statistische Struktur der Meteorologishen Felder*, 364 pp., OMSZ Hiv. Kiadv. XLI Kotet, Budapest.

Entin, J. K., A. Robock, K. Y. Vinnikov, S. Hollinger, S. Liu, and A. Namkhai (2000), Temporal and spatial scales of observed soil moisture variations in the extratropics, *J. Geophys. Res.*, *105*, 11,865–11,877, doi:10.1029/2000JD900051.

Hrda, J. (1968), On statistical structure of surface air temperature field in Czech and Moravia (in Russian), *Idojaras*, *72*(4), 210–215.

Kagan, R. L. (1997), *Averaging of Meteorological Fields*, Kluwer Acad., Dordrecht, Netherlands.

Long, C. N., and T. P. Ackerman (2000), Identification of clear skies from broadband pyranometer measurements and calculation of downwelling shortwave cloud effects, *J. Geophys. Res.*, *105*, 15,609–15,626, doi:10.1029/2000JD900077.

Long, C. N., and D. D. Turner (2008), A method for continuous estimation of clear-sky downwelling longwave radiative flux developed using ARM surface measurements, *J. Geophys. Res.*, *113*, D18206, doi:10.1029/2008JD009936.

Long, C. N., T. P. Ackerman, K. L. Gaustad, and J. N. S. Cole (2006), Estimation of fractional sky cover from broadband shortwave radiometer measurements, *J. Geophys. Res.*, *111*, D11204, doi:10.1029/2005JD006475.

Rakoczi, F., A. Szakacsne, K. Orendi, and K. M. Lugina (1976), Statistische struktur der bodennahen meteorologischen felder, Temperature, in *Statistische Struktur der Meteorologishen Felder*, edited by R. Czelnai, L. S. Gandin, and W. I. Zachariew, pp. 201–234, OMSZ Hiv. Kiadv. XLI Kotet, Budapest.

Razuvaev, V. N., E. G. Apasova, and R. A. Martuganov (2007), Six- and Three-hourly Meteorological Observations from 223 Former U.S.S.R. Stations, doi:10.3334/CDIAC/cli.ndp048, World Data Cent. for All-Russ. Res. Inst. of Hydrometeorol. Inf., Obninsk, Russia.

Snyder, W. C., Z. Wan, Y. Zhang, and Y.-Z. Feng (1998), Classification-based emissivity for land surface temperature measurement from space, *Int. J. Remote Sens.*, *19*, 2753–2774, doi:10.1080/014311698214497.

Ulivieri, C., and G. Cannizzaro (1985), Land surface temperature retrievals from satellite measurements, *Acta Astronaut.*, *12*, 977–985, doi:10.1016/0094-5765(85)90026-8.

van den Dool, H. (2007), *Empirical Methods in Short-Term Climate Prediction*, 215 pp., Oxford Univ. Press, New York.

Vinnikov, K. Y., and N. C. Grody (2003), Global warming trend of mean tropospheric temperature observed by satellites, *Science*, *302*, 269–272, doi:10.1126/science.1087910.

Vinnikov, K. Y., and A. Robock (2002), Trends in moments of climatic indices, *Geophys. Res. Lett.*, *29*(2), 1027, doi:10.1029/2001GL014025.

Vinnikov, K. Y., and I. B. Yeserkepova (1991), Soil moisture: Empirical data and model results, *J. Clim.*, *4*, 66–79, doi:10.1175/1520-0442 (1991)004<0066:SMEDAM>2.0.CO;2.

Vinnikov, K. Y., A. Robock, N. A. Speranskaya, and C. A. Schlosser (1996), Scales of temporal and spatial variability of midlatitude soil moisture, *J. Geophys. Res.*, *101*, 7163–7174, doi:10.1029/95JD02753.

Vinnikov, K. Y., A. Robock, and A. M. Basist (2002), Diurnal and seasonal cycles of trends of surface air temperature, *J. Geophys. Res.*, *107*(D22), 4641, doi:10.1029/2001JD002007.

Vinnikov, K. Y., A. Robock, N. C. Grody, and A. Basist (2004), Analysis of diurnal and seasonal cycles and trends in climatic records with arbitrary observation times, *Geophys. Res. Lett.*, *31*, L06205, doi:10.1029/2003GL019196.

Vinnikov, K. Y., N. C. Grody, A. Robock, R. J. Stouffer, P. D. Jones, and M. D. Goldberg (2006), Temperature trends at the surface and in the troposphere, *J. Geophys. Res.*, *111*, D03106, doi:10.1029/2005JD006392.

Vinnikov, K. Y., Y. Yu, M. K. R. V. Raja, D. Tarpley, and M. D. Goldberg (2008), Diurnal-seasonal and weather-related variations of land surface temperature observed from geostationary satellites, *Geophys. Res. Lett.*, *35*, L22708, doi:10.1029/2008GL035759.

Yu, Y., J. L. Privette, and A. Pinheiro (2008), Evaluation of split-window land surface temperature algorithms for generating climate data records, *IEEE Trans. Geosci. Remote Sens.*, *46*(1), 179–192, doi:10.1109/TGRS.2007.909097.

Yu, Y., D. Tarpley, J. L. Privette, M. K. Rama Varna Raja, K. Y. Vinnikov, and H. Xue (2009), Developing algorithm for operational GOES-R land surface temperature product, *IEEE Trans. Geosci. Remote Sens.*, *47*(3), 936–951, doi:10.1109/TGRS.2008.2006180.

M. Chen, IMSG at NOAA/NESDIS/STAR, 5200 Auth Rd., Camp Springs, MD 20746, USA.

M. D. Goldberg and Y. Yu, NOAA/NESDIS, 5200 Auth Rd., Camp Springs, MD 20746, USA.

D. Tarpley, Short and Associates, Inc., 3307 Rolling Rd., Chevy Chase, MD 20815, USA.

K. Y. Vinnikov, Department of Atmospheric and Oceanic Science, University of Maryland, College Park, MD 20742, USA. (kostya@atmos.umd.edu)